

# Iterative Prompt Relabeling for diffusion model with RLDF

Jiaxin Ge\*  
Peking University

Xinyan Chen\*  
University of Science and Technology of China

Tianjun Zhang\*  
UC Berkeley

Shanghang Zhang<sup>†</sup>  
Peking University

## Abstract

Diffusion models have shown impressive performance in many domains, including image generation, time series prediction, and reinforcement learning. The algorithm demonstrates superior performance over the traditional GAN and transformer based methods. However, the model’s capability to follow natural language instructions (e.g., spatial relationships between objects, generating complex scenes) is still unsatisfactory. This has been an important research area to enhance such capability. Prior works adopt reinforcement learning to adjust the behavior of the diffusion models. However, RL methods not only require careful reward design and complex hyperparameter tuning, but also fails to incorporate rich natural language feedback. In this work, we propose iterative prompt relabeling (IP-RLDF), a novel algorithm that aligns images to text through iterative image sampling and prompt relabeling. IP-RLDF first samples a batch of images conditioned on the text, then relabels the text prompts of unmatched text-image pairs with classifier feedback. We conduct thorough experiments on three different models, including SDv2, GLIGEN, and SDXL, testing their capability to generate images following instructions. With IP-RLDF, we improved up to 15.22% (absolute improvement) on the challenging spatial relation VISOR benchmark, demonstrating superior performance compared to previous RL methods.

## 1. Introduction

Recent advancements in the field of image generation have been notably driven by diffusion models, especially in the area of text-to-image conversion [10, 13, 14, 39, 43]. These models have shown impressive capabilities in creating visually compelling images from descriptive text. However, a significant challenge arises when these models are tasked

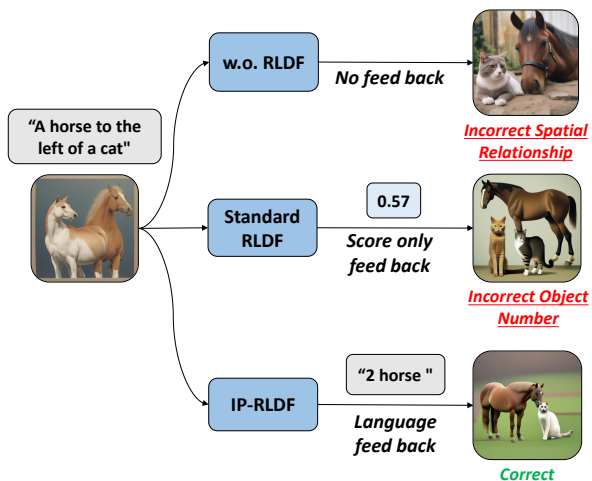


Figure 1. Comparison of the outcomes of fine-tuning diffusion models with score feedback, language feedback, and without any feedback. Models utilizing score feedback and without any feedback exhibit an insufficient understanding of the prompt’s spatial semantics, while employing language feedback significantly improves spatial accuracy of generated images.

with interpreting and executing complex instructions, particularly those involving spatial relationships [10, 40]. One simple example is a prompt like “a dog left to a car” often result in images where the spatial relationship “left to” is not accurately depicted. This limitation underscores a crucial gap in the current models’ ability to understand and render intricate spatial dynamics, which is essential for creating contextually accurate images.

The predominant approach to training diffusion models involves matching a specific data distribution, typically through supervised learning methods [3, 30]. While effective in certain contexts, these methods require a significant amount of human labeling and also fall short when dealing with complex instructions, particularly those requiring an understanding of spatial relationships. Recently, efforts have shifted towards exploring the use of Reinforcement

\*Equal contribution

<sup>†</sup>Corresponding author

<sup>1</sup>Preprint: Work in Progress

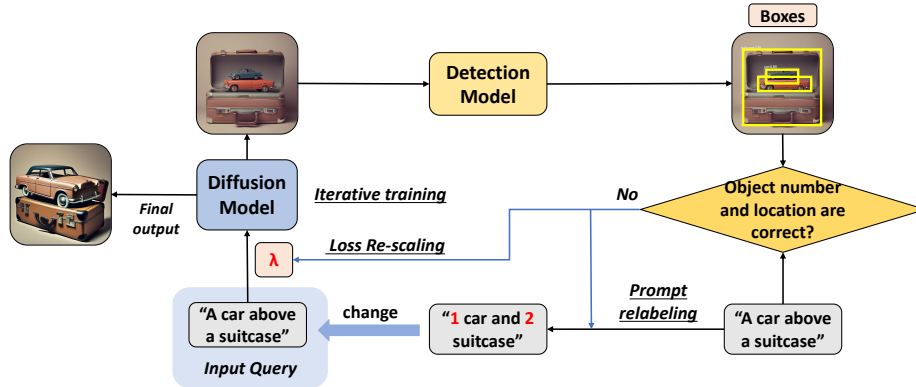


Figure 2. The general pipeline of IP-RLDF. IP-RLDF enhances the alignment of images with text through the combination of RL, prompt relabeling, and iterative training.

Learning (RL)[18, 25] to address these issues. RL offers a distinct advantage in its ability to directly optimize for specific, complex goals, such as accurate spatial representation. Therefore making it more adaptable to nuanced tasks than traditional methods. However, RL-based methods face their own set of challenges, including the need for careful reward design, complicated reward model training, and hyperparameter tuning. Moreover, the only feed back for optimization is a scalar value reward, which fails to efficiently capture the subtleties of rich natural language feedback in the context of text-to-image generation.

In response to these challenges, we propose **Iterative Prompt Relabeling with RL Detection Feedback**(IP-RLDF), a novel technique designed to enhance the alignment of images with text through an iterative process of image sampling and prompt relabeling. Our approach uses rich language feedback and simple reward design. We begin by establishing a reward function based on an external detection model that automatically classifies the correctness of an image and assign rewards based on the detection results. This enables a straightforward reward design and neglect the complicated training of reward models. Then, we use prompt relabeling to relabel the input prompt of the mismatched image-text pairs based on the results of the detection model. Finally, we adopt iterative training that continuously trains the model with its self-generated images. Iterative training allows dynamically scaling up the dataset and receiving additional feedback through multiple training rounds, which can further enrich the feedback and progressively refines the model’s performance.

In our study, we demonstrate the efficacy of IP-RLDF across various settings, including state-of-the-art diffusion models like SDv2[37], GLIGEN[27], and SDXL[33] and test on the challenging spatial relation task, where we observed a substantial improvement of up to 15.22% (absolute improvement) on the VISOR[11] benchmark. This perfor-

mance underlines the potential of IP-RLDF in pushing the boundaries of text-to-image generation models, especially in terms of understanding and rendering complex spatial relationships.

Our contribution can be summarized as follows:

- We propose IP-RLDF, a novel algorithm that incorporates a pipeline of RL, prompt relabeling, and iterative training to address the challenging spatial relationship task. We are the first to integrate the benefits of language signal feedback with the reward design to train text-to-image diffusion models.
- Our algorithm is an additional plug-and-play algorithm that could be integrated across a variety of diffusion model settings. We tested our algorithm across three diffusion models, all showing significant gains.
- We conducted extensive experiments on the spatial relation VISOR benchmark, our proposed algorithm shows a substantial improvement on generating images with correct spatial locations over other algorithms. Showing the effectiveness and potential of this mechanism on training diffusion models.

## 2. Related Works

### 2.1. Diffusion probabilistic models.

Recently, denoising diffusion models have demonstrated robust capabilities as a class of generative models, with applications in domains such as image [9, 35] and video generation [14, 15] and their subsequent processing. They have also exhibited exceptional performance in tasks like audio synthesis[22], robotics[17, 20], and various scientific domains. Training diffusion models typically deviates from the conventional likelihood maximization[13, 32], and as people often pay more attention on downstream objectives, making a rigorous commitment to enhancing probability can often lead to a degradation in image quality[32]. There-

fore, utilizing reinforcement learning techniques to improve diffusion models in our work may be a promising strategy.

## 2.2. Controllable generation with diffusion models

Text-to-image models have facilitated the generation of high-resolution, multi-styled images[35, 40, 48]. However, training diffusion models from scratch demands a substantial amount of data and time. Therefore, various fine-tuning strategies have been explored to extend the potential and enhance the quality of diffusion model generation in specific domains. These approaches include associating a unique identifier with a particular subject [39], introducing new embeddings to represent user-provided concepts [10], adapting compositional generation[31], incorporating input constraint adapters [45], and implementing Low-Rank Adaptation for the Transformer architecture[16]. Our work utilize LoRA to fine-tune diffusion model.

## 2.3. Reinforcement learning

Reinforcement learning has been employed in various tasks. In text-to-image alignment task, diffusion models have been fine-tuning through the maximization of reward-weighted likelihood[23]. Another noteworthy advancement, DDPO[2], has explored reinforcement learning techniques for the direct optimization of diffusion models, achieving a range of objectives, including the integration of human feedback. However, its main approach focuses on numerical rewards, whereas our work places greater emphasis on language feedback.

## 2.4. Prompt relabeling

Recent research has demonstrated the efficacy of prompt relabeling techniques. TEMPERA[46] offers interpretable prompts tailored to various queries through the creation of an innovative action space, enabling flexible adjustments to the initial prompts. Furthermore, the Hindsight Instruction Relabeling (HIR)[47] approach conceptualizes instruction alignment problem as a goal-reaching problem within the context of decision-making. It entails the conversion of feedback into instructions by re-labeling the original instructions. Our approach represents a significant advancement as it employs prompt relabeling techniques with diffusion models for the first time.

## 3. Preliminary

### 3.1. Diffusion Models

Diffusion models are built on the concept of a Markov chain where each step adds Gaussian noise to an image. Formally, the forward diffusion process is represented by:

$$q(x_t|x_{t-1}) = \mathcal{N}(\sqrt{1 - \beta_t}x_{t-1}, \beta_t I) \quad (1)$$

where  $x_t$  is the image at time step  $t$ ,  $\beta_t$  denotes the variance at each step, and  $I$  is the identity matrix. The reverse process involves a neural network  $\mu_\theta(x_t, c, t)$  that gradually denoises the image, incorporating additional contextual parameters  $c$  related to the text description. DDPM [13] parameterized this equation by  $\mu_\theta(x_t, c, t) = \frac{1}{\sqrt{\alpha_t}}(x_t - \frac{\beta_t}{\sqrt{1-\alpha_t}}\epsilon_\theta(x_t, c, t))$ . We usually optimize this objective function by variational lower bound:

$$L_\theta = \mathbb{E}_{x_0, \epsilon, t} [\|\epsilon - \epsilon_\theta(x_t, c, t)\|^2] \quad (2)$$

where  $\epsilon$  is the noise added at each step, and  $\epsilon_\theta$  is the noise predicted by the model.

## 3.2. Reinforcement Learning

In a Markov Decision Process (MDP), we define state space  $S$ , action space  $A$ , and (non-deterministic) transition function  $\mathcal{T} : S \times A \rightarrow P(S)$  where  $P(S)$  is the probability of next state given the current state and action. The goal is to maximize the expected reward  $R = \mathbb{E}[\sum_{k=0}^T \gamma^k r_{t+k=1}]$  where  $r_t$  is the reward and  $\gamma$  is the discount factor. In this paper, the total reward received at time step  $t$  is given by  $r_t = r_t^e + \alpha r_t^i$ , where  $r_t^e$  is the extrinsic reward given by the environment,  $r_t^i$  is the intrinsic reward from the exploration criterion, and  $\alpha$  is a scaling hyperparameter.

## 4. Method

In this section, we provide an overview of our method and a detailed description of each part of our method. Please also refer to the pseudo code in Algorithm 1 for our full method.

---

### Algorithm 1 Iterative Prompt Relabeling with RL Feedback (IP-RLDF)

---

**Require:** Text prompts  $C$ , pretrained model  $\theta$ , detection model  $D$ , iterations  $T$ , data  $X$

**Ensure:** Refined parameters  $\theta'$

- 1: Initialize  $\theta' \leftarrow \theta$
  - 2: **for** iteration = 1 **to**  $T$  **do**
  - 3:    $X_0 \leftarrow \text{Sample\_Images}(\text{Diffusion\_Model}, C, \theta')$
  - 4:   **for** each  $x_0$  in  $X_0$  **do**
  - 5:      $\text{Objects}, \text{Bounding\_Box} \leftarrow D(x_0)$
  - 6:      $\text{Count}, \text{Relation} \leftarrow \text{Analyze}(D)$
  - 7:      $\text{Reward} \leftarrow \text{CalcReward}(\text{Count}, \text{Relation}, C)$
  - 8:      $\lambda \leftarrow (\text{Count}, \text{Relation match } C)?1 : 0.5$
  - 9:      $L_{\text{rescaled}} \leftarrow L_{\text{DDPM}}(x_0, \theta') \times \lambda$
  - 10:      $c_{\text{new}} \leftarrow \text{Relabel}(C, D)$
  - 11:     Update  $X$  with  $(x_0, c_{\text{new}}, L_{\text{rescaled}})$
  - 12:   **end for**
  - 13:    $\theta' \leftarrow \text{TrainModel}(X, \theta')$
  - 14: **end for**
- return**  $\theta'$
-

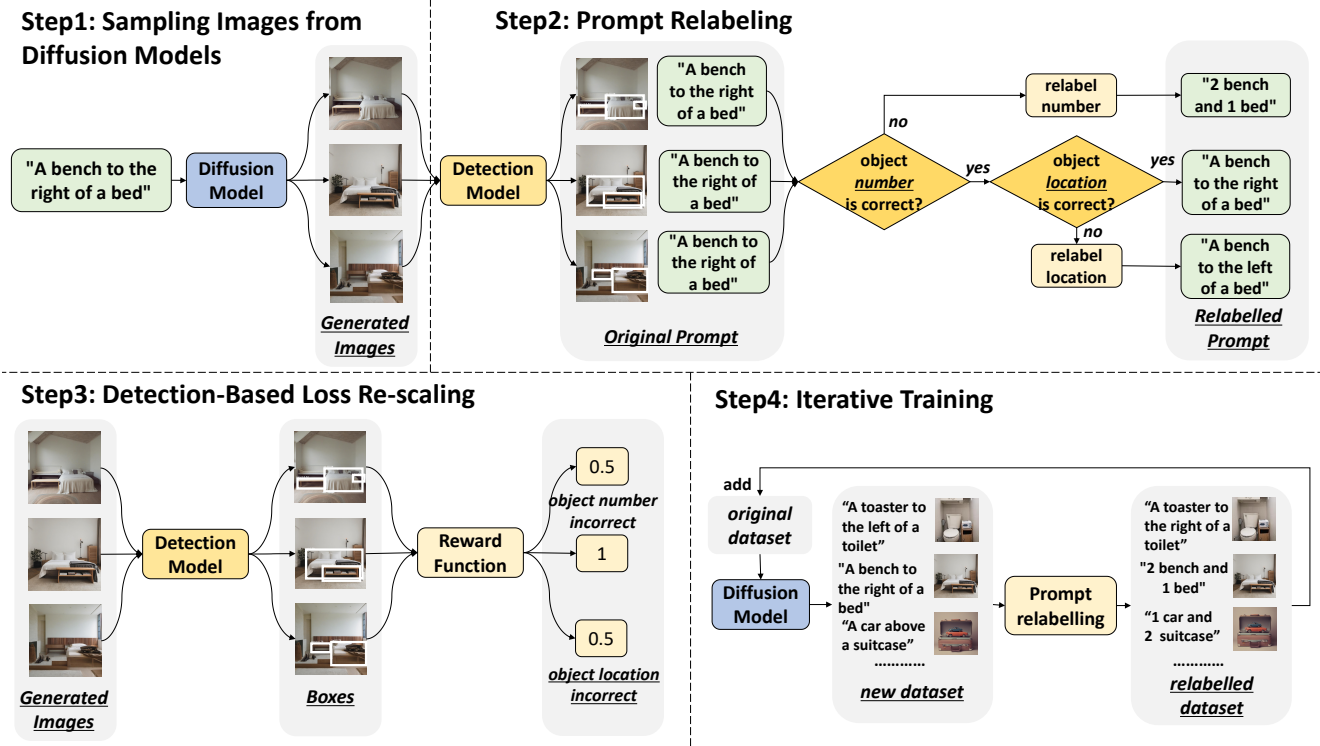


Figure 3. The components of our IP-RLDF algorithm. (1)Sampling Images from Diffusion Models: sample images from a diffusion model conditioned on textual prompt. (2)Prompt Relabeling: detect the generated image to yield a bounding box; analyze the box to modify original prompt. (3)Detection-Based Loss Re-scaling: apply a detection model to rescale the loss function. (4)Iterative Training: retrain the model with updated dataset iterately.

Score Type	Method	SDv2(1)	SDv2(LoRA)	SDXL(LoRA)	SDv2(2)	GLIGEN
Spatial Accuracy(%)	Direct	18.75	18.75	27.00	17.00	14.0
	RLDF	21.50	22.00	29.75	22.44	-
	<b>IP-RLDF</b>	<b>28.50</b>	<b>25.25</b>	<b>31.25</b>	<b>32.22</b>	<b>20.0</b>
CLIP Score	Direct	25.75	25.75	27.41	-	-
	RLDF	<b>26.67</b>	26.09	28.68	-	-
	<b>IP-RLDF</b>	25.87	<b>26.15</b>	<b>28.74</b>	-	-

Table 1. Combined results of spatial accuracy and CLIP score on five settings. (1)Direct: The original diffusion models. (2)RLDF: Only applying RLDF on diffusion models. (3)IP-RLDF: Our method. The results show that IP-RLDF outperforms other methods in generating images with correct spatial relationships.

#### 4.1. Method Overview

We propose a novel framework, IP-RLDF, a reinforcement learning algorithm tailored for comprehending and generating images that adhere to complex spatial relationships expressed in text. Our approach adopts three different stages: diffusion model sampling, detection-based loss adjustment, prompt relabeling, and iterative refinement. This approach is illustrated in Figure 2, first generating a batch of images from diffusion models using text prompts. Then the text and generated image pairs got checked by an RLDF mod-

ule, which gives rich natural language feedback to relabel the original text prompt. Finally, the model is trained on the new relabeled text-image pairs in an iterative manner. We will introduce the details of each stage in the following sections.

#### 4.2. Sampling Images from Diffusion Models

IP-RLDF first samples images from a diffusion model conditioned on textual prompts. We follow the standard image sampling process for diffusion models conditioned on a given text description prompt. The sampling process is

governed by the following equation:

$$p_{\theta}(x_0|c) = \int p_{\theta}(x_0|x_t)p_{\theta}(x_t|c) dt \quad (3)$$

Here,  $x_0$  is the generated image,  $c$  is the text prompt, and  $x_t$  represents intermediate states in the diffusion process. The model parameters  $\theta$  are optimized to maximize the likelihood of generating  $x_0$  that accurately corresponds to  $c$ . The function  $p_{\theta}(x_0|x_t)$  denotes the reverse diffusion process, which iteratively reconstructs the image from the noise, and  $p_{\theta}(x_t|c)$  represents the conditional distribution of the intermediate state given the text prompt.

### 4.3. Prompt Relabeling

The sampled images from the diffusion model consist of the ones that are aligned with the text prompt and the ones that are not. We then relabels the inconsistent image-text pairs to ensure that the textual description accurately reflects the content of the generated image. These data are later on added to the original training set to train the new diffusion model. Although the relabeling process can be general in the language space, for our experiments, we specifically consider consistency regarding the number of objects and their layouts. The algorithm takes the following steps:

1. Detect objects in the generated image using a detection model, yielding bounding boxes (bbox) for each object.
2. Compare the number of detected objects with the object count specified in the original prompt.
3. If the object count matches, analyze the bounding box centers to determine the actual spatial relationship between objects. Modify the original prompt to accurately describe this relationship.
4. If the object count does not match, revise the prompt to reflect the actual number and type of objects in the image (e.g., "2 cats and 1 dog").

This relabeling can be mathematically represented as:

$$c_{\text{new}} = \text{RelabelPrompt}(c, \text{DetectedObjects}, \text{BBoxInfo}) \quad (4)$$

where  $c_{\text{new}}$  is the relabeled prompt, `DetectedObjects` indicates the objects identified by the detection model, and `BBoxInfo` contains the bounding box information used to ascertain spatial relationships.

### 4.4. Detection-Based Loss Re-scaling

We then train the diffusion model with this new relabeled dataset with a rescaled loss function according to their consistency assessment. The loss function is rescaled based on this assessment:

$$L_{\text{rescaled}} = \mathbb{E}_{x_i, c_i} [\lambda_{x_i, c_i} L_{\theta}(x_i, c_i)] \quad (5)$$

where  $L_{\theta}$  is the standard diffusion model loss (Eq. 2). The modulatory factor  $\lambda$  is defined as:

$$\lambda = \begin{cases} 1 & \text{if image is consistent with its text prompt} \\ 0.5 & \text{otherwise} \end{cases} \quad (6)$$

The rescaling factor  $\lambda$  balances the model’s capability to follow text prompts while keep the new generated image distribution is not too far away from its original.

### 4.5. Iterative Training

Like other reinforcement learning approaches, we iteratively sampling from and training the model from its own outputs. The iterative training cycle is the cornerstone of our methodology. Each iteration involves retraining the model with the updated dataset comprising of newly generated images, their corresponding relabeled prompts, and the rescaled loss:

$$\theta_{\text{new}} = \text{Train}(\theta_{\text{old}}, \{(x_0^{(i)}, c_{\text{new}}^{(i)}, L_{\text{rescaled}}^{(i)})\}_{i=1}^N) \quad (7)$$

where  $N$  is the number of samples in each iteration. This iterative process leads to continual improvement in the model’s ability to produce spatially coherent images aligned with textual descriptions.

## 5. Experiments

In this section, we assess the IP-RLDF algorithm’s effectiveness through experiments on multiple diffusion models in different contexts. Our results show that IP-RLDF significantly improves image generation in terms of spatial accuracy over baseline methods.

### 5.1. Experimental Settings

**Settings and Baselines.** Our experiments involve three state-of-the-art pre-trained diffusion models: SDv2 [37], GLIGEN [27], and SDXL [33], chosen for their proven effectiveness in text-to-image tasks. These models have undergone extensive training on large, diverse datasets[41, 42]. For fine-tuning, we conduct five sets of experiment:

1. Unfrozen SDv2 fine-tuning with an initial learning rate of 1e-6, adjusted in later iterations, using Stabilityai/Stable-Diffusion-2-1 as pretrained model.
2. A different SDv2 unfrozen fine-tuning based on Stabilityai/Stable-Diffusion-2-1-Base pretrained model, starting with a 1e-5 learning rate which is decreased as needed.
3. SDv2 LoRA fine-tuning, using Stabilityai/Stable-Diffusion-2-1 as pretrained model, only training the rank decomposition matrices[16] injected into the UNet[38] module and freeze other params. The learning rate is set to 1e-6.

Score Type	Method	SDv2(1)	SDv2(LoRA)	SDXL(LoRA)	SDv2(2)	GLIGEN
Spatial Accuracy(%)	P	24.50	21.50	28.25	-	-
	RLDF	21.50	22.00	29.75	22.44	-
	P-RLDF	25.75	24.25	30.00	25.22	16.8
	<b>IP-RLDF</b>	<b>28.50</b>	<b>25.25</b>	<b>31.25</b>	<b>32.22</b>	<b>20.0</b>

Table 2. Ablation Study on the effect of the three parts of our method (metric: spacial accuracy). We focus on the SDv2 and SDXL setting for ablation and also provide ablation on adding iterative training on GLIGEN. (1)P: Only applying prompt relabeling on diffusion models. (2)RLDF: Only applying RLDF on diffusion models. (3)P-RLDF: Fine-tuning diffusion models with RLDF and prompt relabeling for one iter. (4)IP-RLDF: Iterative training. IP-RLDF consistently achieve higher spatial accuracy in different settings.

Score Type	Method	SDv2(1)	SDv2(LoRA)	SDXL(LoRA)
CLIP Score	P	26.64	26.00	28.81
	RLDF	<b>26.67</b>	26.09	28.68
	P-RLDF	25.86	25.95	<b>29.01</b>
	<b>IP-RLDF</b>	25.87	<b>26.15</b>	28.74

Table 3. Ablation Study on the effect of the three parts of our method (metric: CLIP score), focusing on SDv2 and SDXL settings. The IP-RLDF method does not consistently achieve the highest CLIP score.

- SDXL LoRA fine-tuning, freezing the model but training the rank decomposition matrices injected into the UNet and text-encoder[34] at a  $1e-5$  learning rate.
- Unfrozen GLIGEN fine-tuning with an initial learning rate of  $1e-5$ , decreased in later iterations,

In those five settings, we train 3 epochs for each iter. Moreover, our detection model, GLIPv2[44], is chosen for its superior zero-shot and few-shot object recognition capabilities, demonstrating higher detection accuracy than alternatives.

**Dataset.** From the VISOR benchmark[11], a challenging spatial relation dataset, we select 100 prompts for self-training, and randomly chose 2000 prompts to form our foundational dataset. Initially, our model is trained on all 2100 prompts and their originally generated images. In each following iteration, the model is trained on the 100 self-training prompts with images from the previous iteration, in addition to the original 2000 prompts and their images.

**Metrics.** Our main objective is generating high-quality images with correct spatial relationship. So instead of using the standard metrics that evaluate the aesthetic quality of images, we consider evaluating spatial accuracy. Our spatial accuracy metric is defined by the GLIPv2 detection model. The detection model detects all the objects in the image in the form of (object name, bounding box) pair. Then, it counts whether the object numbers is correct and also whether object’s spatial relationship is correct by comparing the bounding box center of the objects. If the object number and object spatial relation are both correct, the image is classified as correct, if not, then it is classified as incorrect. Beside the spatial accuracy, we also use the standard evaluation metric CLIP score [34]. which evaluates

the text-image matchness based on the similarity between the encoded text vector and the encoded image vector in the latent space. Due to the lack of ground-truth images in this benchmark, we did not test on the metrics that requires a ground-truth image.

## 5.2. Quantitative Results

In Table 1, we provide the results of spatial accuracy and CLIP score across five different settings referred in 5.1. We compared against the standard RLDF training without prompt-relabeling or iterative training.

**Spatial Accuracy Analysis.** The result shows that IP-RLDF significantly outperforms the RLDF baseline across all settings. Specifically, for the SDv2(1) configuration, it achieves a 9.75% improvement in spatial accuracy, and for SDv2(2), up to a 15.22% enhancement. With the GLIGEN model, the IP-RLDF improves spatial accuracy by 6.00%. And in the settings of fine-tuning SDv2 and SDXL with LoRA, improvements are 6.50% and 4.25%, respectively. These results suggest that IP-RLDF is an effective algorithm in training diffusion models to accurately depict spatial relationships, outperforming conventional training without language feedback or iterative processes. The consistent improvement over all settings also verify the method’s robustness in different model training and techniques.

**Text-to-Image Alignment Analysis.** IP-RLDF also demonstrates remarkable gains in CLIP score over both the RLDF algorithm and the original text-to-image models in SDv2(LoRA) and SDXL(LoRA) settings, indicating that it keeps the image’s quality and achieves remarkable text-to-image alignment while enhancing the spatial correctness. One exception occurs during SDv2(1), where the RLDF

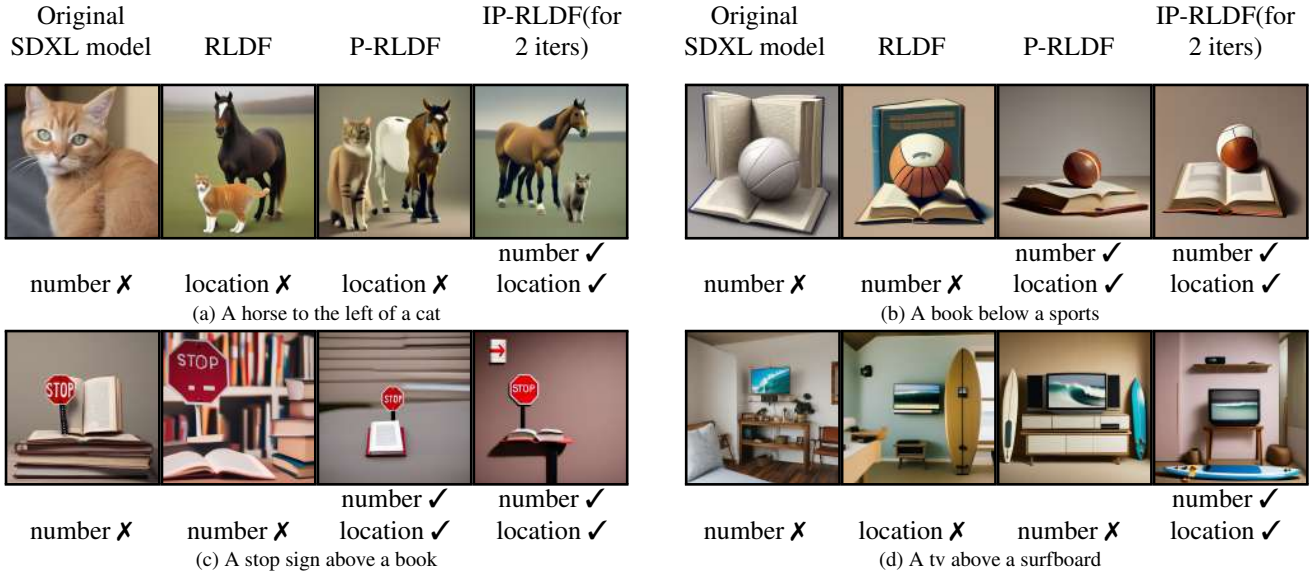


Figure 4. Samples from different models, generated by four distinct prompts. Models are as follows: (1)Using SDXL as the original model. (2)RLDF. (3)P-RLHF. (4)IP-RLDF(trained for two iters). Compared to the original SDXL model, RLDF and P-RLDF methods, our method showcase enhanced spatial awareness and accuracy in generating images of specified objects.

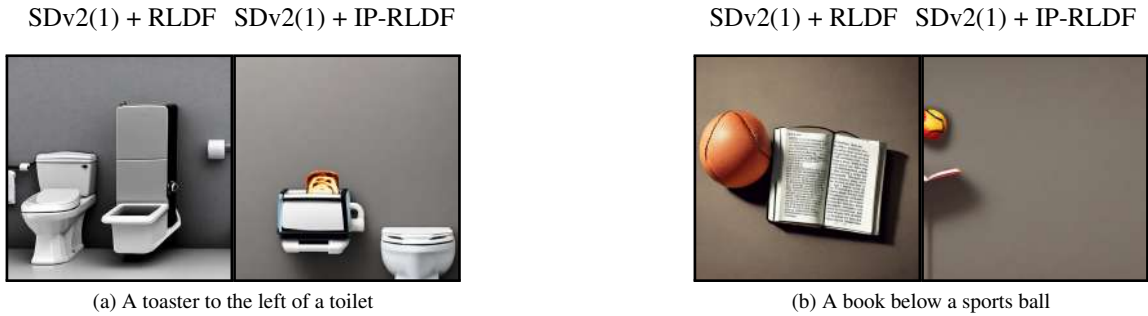


Figure 5. Samples from different fine-tuned models. (1)Left column: unfrozen fine-tuning on sdv2 with RLDF. (2)Right column: unfrozen fine-tuning on SDv2 with IP-RLDF. Compared with RLHF, SDv2 model fine-tuned with IP-RLDF exhibit notable image fidelity but lower spatial accuracy.

outperforms IP-RLDF on CLIP score. This is likely due to a trade-off between spatial accuracy and overall image quality, with IP-RLDF achieving higher spatial accuracy at the expense of a slight decrement in CLIP score. As shown in Figure 5, IP-RLDF blurs and RLDF kept more details, while IP-RLDF shows higher spacial accuracy.

**Training Method Analysis.** The table shows a performance difference between different training techniques. In the LoRA setting, where the weight of pretrained models is frozen and only the rank decomposition matrices injected are trained, the performance gain is less compared with fine-tuning all parameters. However, the LoRA training exhibit notable image fidelity compared with fine-tuning all parameters, as shown in Figure 6. This suggests a trade-off be-

tween enhancing spatial accuracy and keeping overall image quality, indicating possible directions for improvement in future research.

The above results demonstrate that our algorithm is a versatile, plug-and-play solution suitable for diverse diffusion model environments, consistently yielding substantial improvements.

### 5.3. Qualitative Results

Figure 4 provides a visual comparison of the original SDXL model, its fine-tuned versions using RLDF, P-RLDF and IP-RLDF, across four different prompts.

As is demonstrated in figure, The original SDXL model often misinterprets the number and placement of objects, a

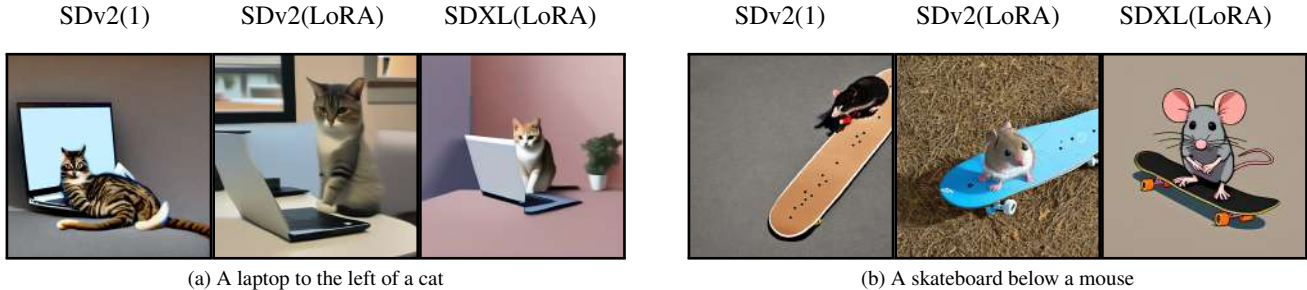


Figure 6. Samples from different models fine-tuned with IP-RLDF, generated by two distinct prompts. (1)Left column: unfrozen fine-tuning on SDv2. (2)Mid column: Utilizing LoRA to fine-tune SDv2. (3)Right column: Utilizing LoRA to fine-tune SDXL. The LoRA training exhibit notable image fidelity than unfrozen training.

Spacial Accuracy (%)	Method	SDv2(1)	SDv2(LoRA)	SDXL(LoRA)
Left-right	Direct	20.63	20.63	25.00
	P	20.63	16.88	30.63
	RLDF	18.13	18.75	28.13
	P-RLDF	20.00	22.50	29.38
	<b>IP-RLDF</b>	<b>26.25</b>	<b>23.13</b>	<b>36.25</b>
Above-below	Direct	17.50	17.50	28.33
	P	27.08	24.58	26.67
	RLDF	23.75	24.17	<b>30.83</b>
	P-RLDF	29.58	25.42	30.42
	<b>IP-RLDF</b>	<b>30.00</b>	<b>26.67</b>	27.92
Object number	Direct	46.75	46.75	51.00
	P	53.00	48.75	54.75
	RLDF	46.75	48.00	56.50
	P-RLDF	52.75	47.75	51.50
	<b>IP-RLDF</b>	<b>58.75</b>	<b>49.75</b>	<b>58.25</b>

Table 4. Different kinds of spacial accuracy of our model and baselines (left-right, above-below and object number), showing that that IP-RLDF outperforms other baselines in recognizing a variety of spatial positional relationships, even though there are minor fluctuations in the above-below spatial relationship of fine-tuned SDXL model.

challenge also seen with RLDF fine-tuning. In contrast, it is evident that our algorithm outperforms both RLDF and the original SDXL model in these aspects, showcasing enhanced spatial awareness and accuracy in depicting the specified objects, while sacrificing some details.

#### 5.4. Ablation Study

**Method Breakdown.** In Table 2 and Table 3, we conduct an ablation study to assess the impact of the three components of our method, focusing on SDv2 and SDXL settings. Additionally, we evaluate the effect of incorporating iterative training into the GLIGEN model. The data clearly show that each component is essential to our algorithm’s performance. Both prompt relabeling and iterative training significantly improves RLDF outcomes. Concurrently, fluctuations are observed within CLIP scores. IP-RLDF does not uniformly reach the highest CLIP scores, which may be at-

tributed to the trade-off between spatial accuracy and image fidelity. For a detailed analysis of the underlying reasons, see Section 5.2.

**Spacial Relationship Type Study.** To further investigate how our algorithm performs across a variety of spatial relationships, we apply an ablation study to different spatial relationships, with a focus on the SDv2 and SDXL models. The findings, detailed in Table 4, revealing that our model consistently outperforms the baseline across diverse spatial relationships. An exception is observed in the ‘above-below’ relationship when fine-tuned on the SDXL model, which may be because the SDXL pretrained model already performs well in spacial accuracy, leaving limited room for IP-RLDF’s enhancements, which results in some fluctuations. However, these fluctuations are within acceptable bounds, meanwhile indicating potential approaches for the algorithm’s refinement.



## 6. Conclusion

In this work, we present IP-RLDF in response to the challenging task of spatial location generation. IP-RLDF is a novel algorithm that designs automatic reward through detection model and incorporates rich language feedback with the rewards. Then it trains the diffusion model by iteratively receiving rewards and language feedbacks. This algorithm is a plug-and-play method that is applicable to a range of diffusion models. And extensive results show the model’s effectiveness on the challenging spatial relationship benchmark across various settings. Our work shows the potential of combining language feedback to reward design as well as the importance of receiving natural language feedback to train text-to-image diffusion models.

## References

- [1] Aishwarya Agrawal, Jiasen Lu, Stanislaw Antol, Margaret Mitchell, C. Lawrence Zitnick, Dhruv Batra, and Devi Parikh. Vqa: Visual question answering, 2016. 2
- [2] Kevin Black, Michael Janner, Yilun Du, Ilya Kostrikov, and Sergey Levine. Training diffusion models with reinforcement learning, 2023. 3
- [3] Tim Brooks, Aleksander Holynski, and Alexei A Efros. Instructpix2pix: Learning to follow image editing instructions. In *Proceedings of the IEEE/CVF Conference on Computer Vision and Pattern Recognition*, pages 18392–18402, 2023. 1
- [4] Maxime Bucher, Tuan-Hung Vu, Matthieu Cord, and Patrick Pérez. Zero-shot semantic segmentation, 2019. 3
- [5] Holger Caesar, Jasper Uijlings, and Vittorio Ferrari. Cocomstuff: Thing and stuff classes in context, 2018. 2
- [6] Nicolas Carion, Francisco Massa, Gabriel Synnaeve, Nicolas Usunier, Alexander Kirillov, and Sergey Zagoruyko. End-to-end object detection with transformers, 2020. 3
- [7] Kai Chen, Jiaqi Wang, Jiangmiao Pang, Yuhang Cao, Yu Xiong, Xiaoxiao Li, Shuyang Sun, Wansen Feng, Ziwei Liu, Jiarui Xu, Zheng Zhang, Dazhi Cheng, Chenchen Zhu, Tianheng Cheng, Qijie Zhao, Buyu Li, Xin Lu, Rui Zhu, Yue Wu, Jifeng Dai, Jingdong Wang, Jianping Shi, Wanli Ouyang, Chen Change Loy, and Dahua Lin. Mmdetection: Open mmlab detection toolbox and benchmark, 2019. 3
- [8] Xinlei Chen, Hao Fang, Tsung-Yi Lin, Ramakrishna Vedantam, Saurabh Gupta, Piotr Dollar, and C. Lawrence Zitnick. Microsoft coco captions: Data collection and evaluation server, 2015. 2
- [9] Prafulla Dhariwal and Alex Nichol. Diffusion models beat gans on image synthesis, 2021. 2
- [10] Rinon Gal, Yuval Alaluf, Yuval Atzmon, Or Patashnik, Amit H. Bermano, Gal Chechik, and Daniel Cohen-Or. An image is worth one word: Personalizing text-to-image generation using textual inversion, 2022. 1, 3
- [11] Tejas Gokhale, Hamid Palangi, Besmira Nushi, Vibhav Vineet, Eric Horvitz, Ece Kamar, Chitta Baral, and Yezhou Yang. Benchmarking spatial relationships in text-to-image generation, 2023. 2, 6
- [12] Agrim Gupta, Piotr Dollár, and Ross Girshick. Lvis: A dataset for large vocabulary instance segmentation, 2019. 3
- [13] Jonathan Ho, Ajay Jain, and Pieter Abbeel. Denoising diffusion probabilistic models, 2020. 1, 2, 3
- [14] Jonathan Ho, William Chan, Chitwan Saharia, Jay Whang, Ruiqi Gao, Alexey Gritsenko, Diederik P. Kingma, Ben Poole, Mohammad Norouzi, David J. Fleet, and Tim Salimans. Imagen video: High definition video generation with diffusion models, 2022. 1, 2
- [15] Jonathan Ho, Tim Salimans, Alexey Gritsenko, William Chan, Mohammad Norouzi, and David J. Fleet. Video diffusion models, 2022. 2
- [16] Edward J. Hu, Yelong Shen, Phillip Wallis, Zeyuan Allen-Zhu, Yuanzhi Li, Shean Wang, Lu Wang, and Weizhu Chen. Lora: Low-rank adaptation of large language models, 2021. 3, 5, 1
- [17] Michael Janner, Yilun Du, Joshua B. Tenenbaum, and Sergey Levine. Planning with diffusion for flexible behavior synthesis, 2022. 2
- [18] L. P. Kaelbling, M. L. Littman, and A. W. Moore. Reinforcement learning: A survey, 1996. 2
- [19] Aishwarya Kamath, Mannat Singh, Yann LeCun, Gabriel Synnaeve, Ishan Misra, and Nicolas Carion. Mdetr – modulated detection for end-to-end multi-modal understanding, 2021. 3
- [20] Ivan Kapelyukh, Vitalis Vosylius, and Edward Johns. Dalle-bot: Introducing web-scale diffusion models to robotics. *IEEE Robotics and Automation Letters*, 8(7):3956–3963, 2023. 2
- [21] Ryan Kiros, Ruslan Salakhutdinov, and Richard S. Zemel. Unifying visual-semantic embeddings with multimodal neural language models, 2014. 2
- [22] Zhifeng Kong, Wei Ping, Jiayi Huang, Kexin Zhao, and Bryan Catanzaro. Diffwave: A versatile diffusion model for audio synthesis, 2021. 2
- [23] Kimin Lee, Hao Liu, Moonkyung Ryu, Olivia Watkins, Yuqing Du, Craig Boutilier, Pieter Abbeel, Mohammad Ghavamzadeh, and Shixiang Shane Gu. Aligning text-to-image models using human feedback, 2023. 3
- [24] Liunian Harold Li, Pengchuan Zhang, Haotian Zhang, Jianwei Yang, Chunyuan Li, Yiwu Zhong, Lijuan Wang, Lu Yuan, Lei Zhang, Jenq-Neng Hwang, Kai-Wei Chang, and Jianfeng Gao. Grounded language-image pre-training, 2022. 2, 3
- [25] Yuxi Li. Deep reinforcement learning: An overview, 2018. 2
- [26] Yiting Li, Haiyue Zhu, Yu Cheng, Wenxin Wang, Chek Sing Teo, Cheng Xiang, Prahlad Vadakkepat, and Tong Heng Lee. Few-shot object detection via classification refinement and distractor retreatment. In *Proceedings of the IEEE/CVF Conference on Computer Vision and Pattern Recognition (CVPR)*, pages 15395–15403, 2021. 3
- [27] Yuheng Li, Haotian Liu, Qingyang Wu, Fangzhou Mu, Jianwei Yang, Jianfeng Gao, Chunyuan Li, and Yong Jae Lee. Gligen: Open-set grounded text-to-image generation, 2023. 2, 5, 1

- [28] Tsung-Yi Lin, Michael Maire, Serge Belongie, Lubomir Bourdev, Ross Girshick, James Hays, Pietro Perona, Deva Ramanan, C. Lawrence Zitnick, and Piotr Dollár. Microsoft coco: Common objects in context, 2015. [2](#)
- [29] Tsung-Yi Lin, Priya Goyal, Ross Girshick, Kaiming He, and Piotr Dollár. Focal loss for dense object detection, 2018. [3](#)
- [30] Haotian Liu, Chunyuan Li, Qingyang Wu, and Yong Jae Lee. Visual instruction tuning. *arXiv preprint arXiv:2304.08485*, 2023. [1](#)
- [31] Nan Liu, Shuang Li, Yilun Du, Antonio Torralba, and Joshua B. Tenenbaum. Compositional visual generation with composable diffusion models, 2023. [3](#)
- [32] Alex Nichol and Prafulla Dhariwal. Improved denoising diffusion probabilistic models, 2021. [2](#)
- [33] Dustin Podell, Zion English, Kyle Lacey, Andreas Blattmann, Tim Dockhorn, Jonas Müller, Joe Penna, and Robin Rombach. Sdxl: Improving latent diffusion models for high-resolution image synthesis, 2023. [2](#), [5](#), [1](#)
- [34] Alec Radford, Jong Wook Kim, Chris Hallacy, Aditya Ramesh, Gabriel Goh, Sandhini Agarwal, Girish Sastry, Amanda Askell, Pamela Mishkin, Jack Clark, Gretchen Krueger, and Ilya Sutskever. Learning transferable visual models from natural language supervision, 2021. [6](#), [1](#)
- [35] Aditya Ramesh, Mikhail Pavlov, Gabriel Goh, Scott Gray, Chelsea Voss, Alec Radford, Mark Chen, and Ilya Sutskever. Zero-shot text-to-image generation, 2021. [2](#), [3](#)
- [36] Joseph Redmon, Santosh Divvala, Ross Girshick, and Ali Farhadi. You only look once: Unified, real-time object detection. In *2016 IEEE Conference on Computer Vision and Pattern Recognition (CVPR)*, pages 779–788, 2016. [3](#)
- [37] Robin Rombach, Andreas Blattmann, Dominik Lorenz, Patrick Esser, and Björn Ommer. High-resolution image synthesis with latent diffusion models, 2022. [2](#), [5](#), [1](#)
- [38] Olaf Ronneberger, Philipp Fischer, and Thomas Brox. U-net: Convolutional networks for biomedical image segmentation, 2015. [5](#), [1](#)
- [39] Nataniel Ruiz, Yuanzhen Li, Varun Jampani, Yael Pritch, Michael Rubinstein, and Kfir Aberman. Dreambooth: Fine tuning text-to-image diffusion models for subject-driven generation, 2023. [1](#), [3](#)
- [40] Chitwan Saharia, William Chan, Saurabh Saxena, Lala Li, Jay Whang, Emily Denton, Seyed Kamyar Seyed Ghasemipour, Burcu Karagol Ayan, S. Sara Mahdavi, Rapha Gontijo Lopes, Tim Salimans, Jonathan Ho, David J Fleet, and Mohammad Norouzi. Photorealistic text-to-image diffusion models with deep language understanding, 2022. [1](#), [3](#)
- [41] Christoph Schuhmann, Richard Vencu, Romain Beaumont, Robert Kaczmarczyk, Clayton Mullis, Aarush Katta, Theo Coombes, Jenia Jitsev, and Aran Komatsuzaki. Laion-400m: Open dataset of clip-filtered 400 million image-text pairs, 2021. [5](#)
- [42] Christoph Schuhmann, Romain Beaumont, Richard Vencu, Cade Gordon, Ross Wightman, Mehdi Cherti, Theo Coombes, Aarush Katta, Clayton Mullis, Mitchell Wortsman, Patrick Schramowski, Srivatsa Kundurthy, Katherine Crowson, Ludwig Schmidt, Robert Kaczmarczyk, and Jenia Jitsev. Laion-5b: An open large-scale dataset for training next generation image-text models, 2022. [5](#), [1](#)
- [43] Yang Song, Prafulla Dhariwal, Mark Chen, and Ilya Sutskever. Consistency models. 2023. [1](#)
- [44] Haotian Zhang, Pengchuan Zhang, Xiaowei Hu, Yen-Chun Chen, Liunian Harold Li, Xiyang Dai, Lijuan Wang, Lu Yuan, Jenq-Neng Hwang, and Jianfeng Gao. Glipv2: Unifying localization and vision-language understanding, 2022. [6](#), [2](#), [3](#)
- [45] Lvmin Zhang, Anyi Rao, and Maneesh Agrawala. Adding conditional control to text-to-image diffusion models, 2023. [3](#)
- [46] Tianjun Zhang, Xuezhi Wang, Denny Zhou, Dale Schuurmans, and Joseph E. Gonzalez. Tempera: Test-time prompting via reinforcement learning, 2022. [3](#)
- [47] Tianjun Zhang, Fangchen Liu, Justin Wong, Pieter Abbeel, and Joseph E. Gonzalez. The wisdom of hindsight makes language models better instruction followers, 2023. [3](#)
- [48] Tianjun Zhang, Yi Zhang, Vibhav Vineet, Neel Joshi, and Xin Wang. Controllable text-to-image generation with gpt-4. *arXiv preprint arXiv:2305.18583*, 2023. [3](#)

# Iterative Prompt Relabeling for diffusion model with RLDF

## Supplementary Material

### A. Overview

Our supplementary material is structured as follows:

- Supplementary experimental details
  - Additional experiments on GLIGEN.
    - \* GLIGEN full results.
    - \* GLIGEN spatial accuracy result.
  - Detailed base models and their fine-tuning methods.
    - \* Stable Diffusion v2 (SDv2).
    - \* Stable Diffusion XL (SDXL).
    - \* Grounded-Language-to-Image-Generation (GLIGEN).
  - Detailed training introduction.
  - Difference between five fine-tuning settings.
  - Detailed detection model introduction.
  - Additional visualization results.
- Additional related works.
  - Detection model.
- Video demonstration.

### B. Supplementary Experimental Details

#### B.1. Additional experiments on GLIGEN

In this section, we focus on the experiments on GLIGEN setting, to validate the effectiveness of our model against different diffusion models. In Table 6, we present full results of spacial accuracy, highlighting that IP-RLDF outperforms other methods in generating images with correct spatial relationships. Moreover, P-RLDF exhibits moderate spatial accuracy and text-to-image alignment. It is evident that the distinctive components of IP-RLDF play an irreplaceable role. In Table 7, we showcase different kinds of spacial accuracy of our GLIGEN fin-tuned model. Notably, P-RLDF outperforms various baselines in a variety of spatial positional relationships, particularly excelling in left-right spatial relations and number accuracy. However, there are minor disparities in the above-below spatial relation, as previously discussed in our spatial relationship experiments.

#### B.2. Detailed base models and their fine-tuning methods

##### B.2.1 Stable Diffusion v2 (SDv2)

Similar to Imagen[14], Stable Diffusion[37] is a latent text-to-image model, with a frozen CLIP ViT-L/14 text encoder[34] and an 860M UNet[38] constructure. This model was pretrained on 256\*256 images followed by fine-tuning on 512\*512 images sourced from the LAION 5B

dataset[42]. It excelled in text-to-image tasks, while concurrently supporting image-to-image tasks.

Stable Diffusion 2.0, however, employs OpenCLIP-ViT/H as its text encoder, which is trained from scratch. In our experiments, we use Stabilityai/stable-diffusion-2-1-base (512\*512 resolution) and Stabilityai/stable-diffusion-2-1 (768\*768 resolution) as base models, both fine-tuned on Stable Diffusion 2.0.

##### B.2.2 Stable Diffusion XL (SDXL)

Compared to the previous stable diffusion models, Stable Diffusion XL[33] features a UNet that is three times larger and integrates OpenCLIP ViT-bigG/14 with the original text encoder. It also introduces crop-conditioning and a two-stage model process to significantly enhance the quality of generated images. Stable Diffusion XL demonstrates improved support for shorter prompts and glyph in images.

##### B.2.3 Grounded-Language-to-Image-Generation (GLIGEN)

GLIGEN[27] is a text-to-image model that incorporates conditional grounding inputs for fine-tuning pre-existing pretrained text-to-image diffusion models, achieving optimal layout-to-image performance. It freezes all the weights of the pretrained model and introduces a new gated self-attention layer between each original self-attention layer and cross-attention layer. Information from caption tokens or grounding tokens can be integrated into the injected gated self-attention layer.

In our experiments, we utilize Gligen/Gligen-generation-text-box as the pretrained model, subsequently training it with bounding boxes generated by our detection model. During inference, no location information is provided. This strategy enables us to showcase the effectiveness of our method by enhancing the performance of the foundational GLIGEN model.

##### B.3. Detailed training introduction

**Low-Rank Adaptation (LoRA).** Due to the considerable time and computational resources required for full fine-tuning of large models, Low-Rank Adaptation[16] was introduced for fine-tuning in particular tasks. It involves injecting rank decomposition matrices into transformer layers while freezing all other model weights. LoRA attains training quality comparable to full fine-tuning but in less time and with fewer computational resources. Initially deployed in large language models, LoRA can also be extended to

Settings	Pretrained models	Unfrozen parts	Resolution	Initial lr	Spatial acc(%)
SDv2(1)	Stabilityai/stable-diffusion-2-1	Full weights	768	1e-6	28.50/18.75
SDv2(LoRA)	Stabilityai/stable-diffusion-2-1	Low-Rank Adaptation	768	1e-6	25.25/18.75
SDXL(LoRA)	Stabilityai/stable-diffusion-xl-base-1.0	Low-Rank Adaptation	1024	1e-5	31.25/27.00
SDv2(2)	Stabilityai/stable-diffusion-2-1-base	Full weights	512	1e-5	<b>32.22/17.00</b>
GLIGEN	Gligen/gligen-generation-text-box	Gated self-attention layer	512	1e-6	20.00/14.00

Table 5. Comparison between five settings, from five different aspects: (1)Pretrained models. (2)Unfrozen parts of each model during fine-tuning. (3)Resolution of models. (4)The initial learning rate of iterative training. (5)Spacial accuracy improvement of different settings. Unfrozen fine-tuning of SDv2 exhibits the most significant improvement in spatial accuracy metrics, and attains the highest spatial accuracy value after fine-tuning.

Score Type	Method	GLIGEN
Spacial Accuracy(%)	Direct	14.00
	P	15.00
	RLDF	14.75
	P-RLDF	17.50
	<b>IP-RLDF</b>	<b>20.00</b>
CLIP Score	P	23.30
	RLDF	23.29
	<b>P-RLDF</b>	<b>23.42</b>

Table 6. Results of spacial accuracy and CLIP score on GLIGEN setting. (1)Direct: The original diffusion models. (2)RLDF: Only applying RLDF on diffusion models. (3)IP-RLDF: Our method. The results show that IP-RLDF outperforms other methods in generating images with correct spatial relationships, and P-RLDF also demonstrates moderate spatial accuracy and text-to-image alignment.

cross-attention layers in text-to-image models such as Stable Diffusion, where it has demonstrated outstanding.

In our experiments, we implement LoRA fine-tuning in SDv2 and SDXL, validating that our IP-RLDF algorithm serves as an additional plug-and-play algorithm capable of integration across various diffusion model settings.

#### B.4. Difference between five fine-tuning settings

In our five fine-tuning settings, we employ the previously mentioned models and fine-tuning methods. Detailed differences among settings are presented in Table 5. Among five settings of experiments, unfrozen fine-tuning of SDv2 exhibits the most significant improvement in spatial accuracy metrics, and attains the highest spatial accuracy value after fine-tuning.

#### B.5. Detailed detection model introduction

GLIPv2[44], a grounded Vision-Language(VL) understanding model, integrates localization[5, 28] and VL understanding[1, 8, 21] to establish grounded VL understanding. It achieves this by innovatively transforming localization tasks into a concentration of category names

Spatial Accuracy (%)	Method	GLIGEN
Left-right	P	13.13
	RLDF	10.63
	<b>P-RLDF</b>	<b>18.75</b>
Above-below	P	16.3
	<b>RLDF</b>	<b>17.50</b>
	P-RLDF	16.67
Object number	P	34.25
	RLDF	35.50
	<b>P-RLDF</b>	<b>37.25</b>

Table 7. Different kinds of spacial accuracy of our GLIGEN fin-tuned model (left-right, above-below and object number), showing that that P-RLDF outperforms other baselines in recognizing a variety of spatial positional relationships.

within VL understanding[24]. This innovative approach effectively resolves the conflicting output format requirements between localization and VL understanding, allowing them to help each other mutually. Consequently, it attains outstanding performance in both localization and understanding tasks. Leveraging its outstanding zero-shot detection capability, we employ the pre-trained GLIPv2 model as the detection component in our framework, yielding excellent results.

#### B.6. Additional visualization results

We showcase qualitative samples from original models and models fine-tuned with various methods (RLDF, P-RLDF, and IP-RLDF). In comparison to the original models, RLDF, and P-RLDF methods, the IP-RLDF method notably demonstrates superior spatial accuracy. Figure 7 shows samples from SDv2 LoRA fine-tuning models; Figure 8 shows samples from SDv2 unfrozen fine-tuning models; Figure 9 shows additional samples from SDv2 unfrozen fine-tuning models. Images in each figure are generated by ten distinct prompts.

## **C. Additional Related Works**

### **C.1. Detection model**

Many studies have concentrated on object detection tasks[6, 7, 29, 36], while the ability to detect certain rare objects[12] still lacks proficiency. Recent work aims to address this issue, adopting novel approaches such as zero-shot[4], few-shot[26], or weakly-supervised[4] methods. Notably, MEDTER[19], GLIP[24], and GLPv2[44] introduce an innovative perspective by transforming object detection tasks into grounded Vision-Language tasks. This integration of Vision-Language aspects into object detection yields remarkable effects in tasks like few-shot object detection. Thus, in our approach, we employ GLPv2 as our chosen detection model within the pipeline.

### **D. Video Demonstration**

We provide a video demonstration, which is available in the attached MP4 file. It explains the motivation behind our IP-RLDF method, outlines the pipeline of our algorithm, and presents qualitative visualization results.

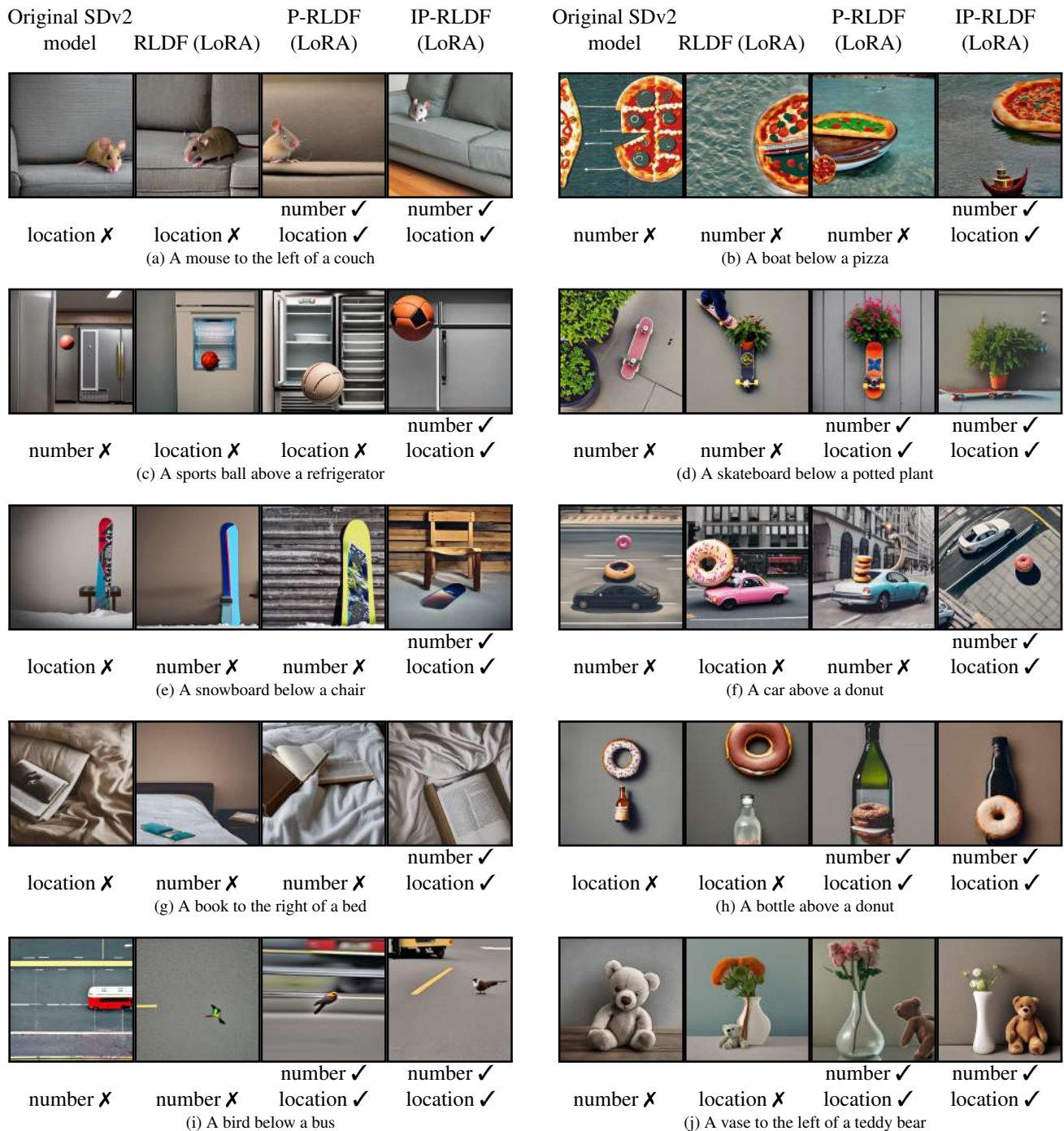


Figure 7. Samples from different models, generated by ten distinct prompts. Models are as follows: (1)Using SDv2 as the original model. (2)RLDF(LoRA fine-tuning). (3)P-RLDF(LoRA fine-tuning). (4)IP-RLDF(trained for two iters, LoRA fine-tuning). Compared to the original SDv2 model, RLDF and P-RLDF methods, our method showcase enhanced spatial awareness and accuracy in generating images of specified objects.

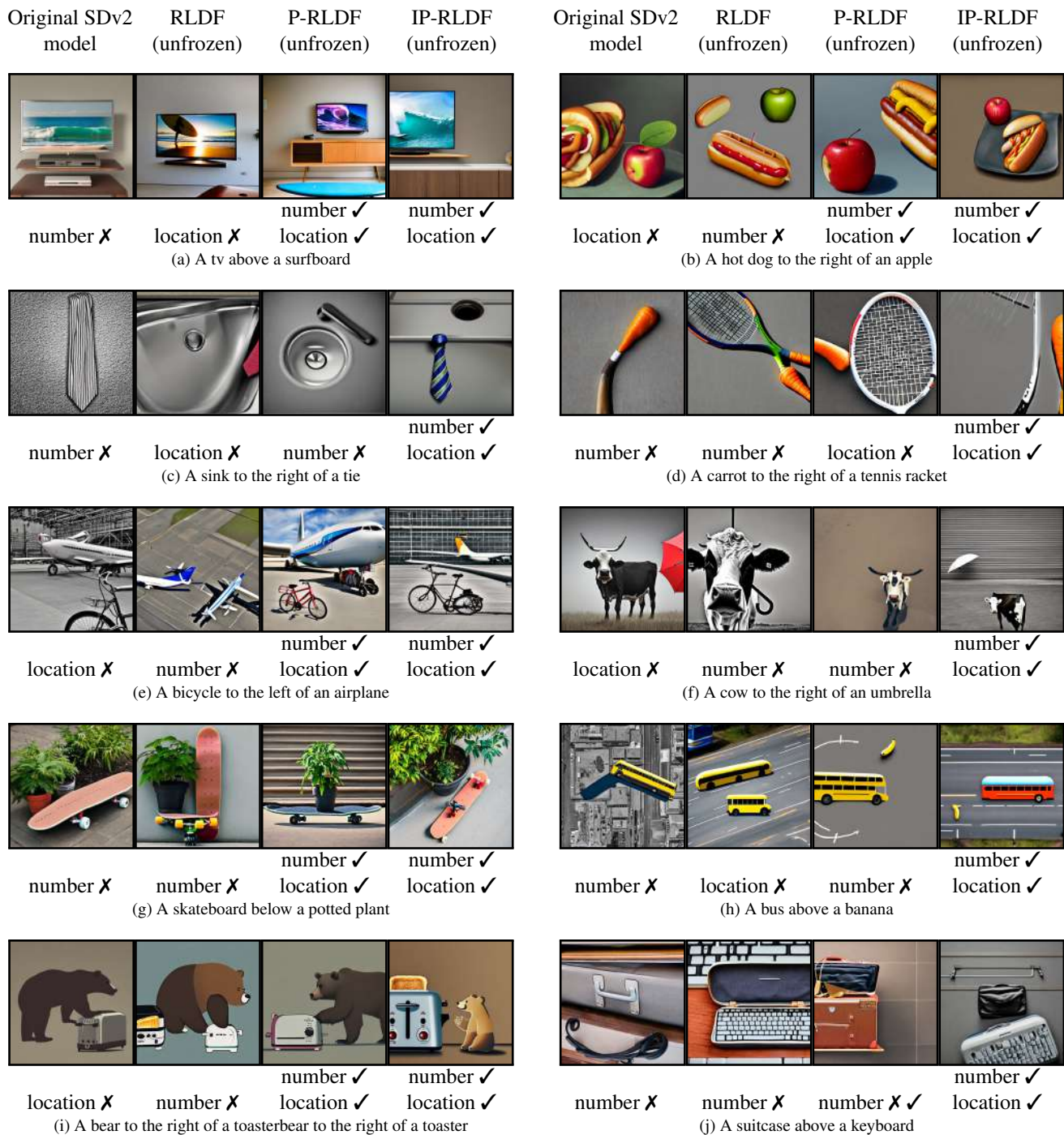


Figure 8. Samples from different models, generated by ten distinct prompts. Models are as follows: (1)Using SDv2 as the original model. (2)RLDF(unfrozen fine-tuning). (3)P-RLDF(unfrozen fine-tuning). (4)IP-RLDF(trained for two iters, unfrozen fine-tuning). Compared to the original SDv2 model, RLDF and P-RLDF methods, our method showcase enhanced spatial awareness and accuracy in generating images of specified objects.

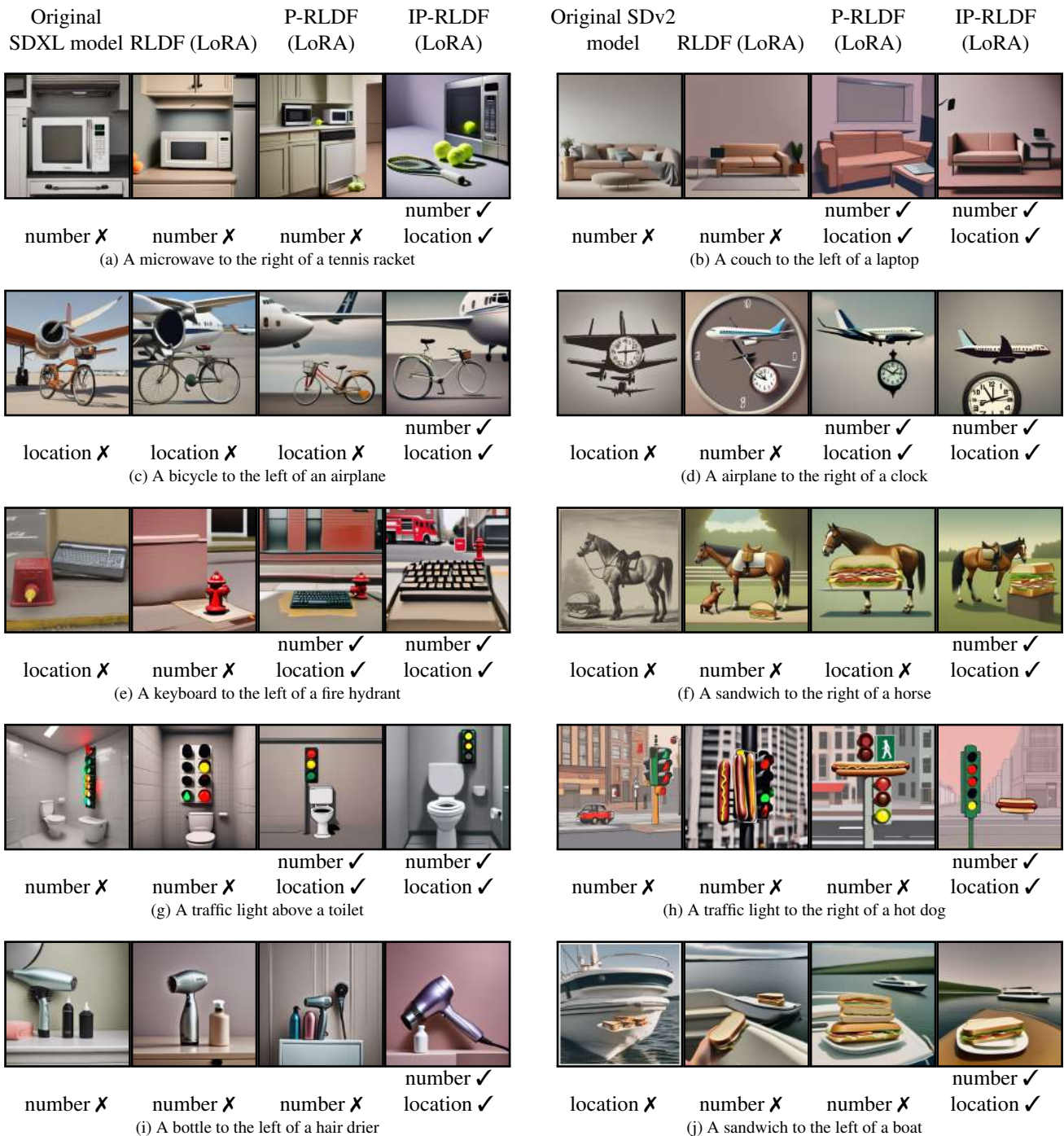


Figure 9. Samples from different models, generated by ten distinct prompts. Models are as follows: (1)Using SDXL as the original model. (2)RLDF(LoRA fine-tuning). (3)P-RLDF(LoRA fine-tuning). (4)IP-RLDF(trained for two iters, LoRA fine-tuning). Compared to the original SDXL model, RLDF and P-RLDF methods, our method showcase enhanced spatial awareness and accuracy in generating images of specified objects.